LAWRENCE
LIVERMORE
NATIONAL
LABORATORY

LLNL-JRNL-819834

Smart Meters Enabling Voltage Monitoring and Control: The Last-Mile Voltage Stability Issue

N. Duan, C. Huang, C. C. Sun, L. Min, C. Applegate, P. Barnes, E. Stewart

February 24, 2021

IEEE Transactions on Industrial Informatics

Disclaimer

Smart Meters Enabling Voltage Monitoring and Control: The Last-Mile Voltage Stability Issue

Nan Duan, Can Huang, Chih-Che Sun, and Liang Min

***Abstract*—This work investigates the voltage monitoring and control feature for smart meters and identifies the impact of this feature on both power distribution and communication systems. Regarding the voltage monitoring, a co-simulation platform is developed using GridLAB-D and ns-3 to analyze the impact of adding voltage measurements to smart meter readings and assess the mitigation strategies for reducing timeout errors and packet drops of smart meter data. Regarding the voltage control, a new voltage stability control scheme is developed, which applies the voltage stability margin as the control objective, instead of the traditional voltage magnitude. The proposed control scheme makes use of existing advanced metering infrastructure (AMI) and distributed energy resources (DERs), requiring small marginal costs. It is indicated that integrating the voltage monitoring and control feature, smart meters could enable the voltage stability issues being solved at end-user sides, i.e., the "last-mile" segment. It is also implied that the new feature could support the coordination of the local and system-level voltage controls using both customer-owned and utility-scale DERs.**

***Index Terms*—smart meter, advanced metering infrastructure, voltage measurement, voltage stability, co-simulation, distributed energy resource, controllable load.**

I. Introduction

SMART meters are an electronic device that performs measurement of electric energy consumption and provides two-way communication between electricity suppliers and customers for customer billing and system monitoring. Compared with conventional electricity meters, smart meters presents several advantages for both utilities and customers, such as higher accuracy, lower cost, better visibility, and greener energy consumption [1]–[3]. For those economic and environmental benefits, an increasing number of smart meters have been deployed around the world. For instance, in the United States, it is reported that about 70 million smart meters were installed from 2007 to 2016 [2], and a total of 90 million smart meters will be invested by 2020, covering about 70% of the electricity customers in the United States [3].

Recently, several review papers well summarized the functions, applications, and technology trends of smart meters [2]–[5], as shown in Fig. 1. They point out that it is advantageous to report energy consumption, together with real power, reactive power, and voltage measurements, such that smart meter data can be used for not only "load" billing and motioning, but also "grid edge" situational awareness [6]; and it is also beneficial to explore new applications that extend the application scope from billing and monitoring

This work was supported by the U.S. Department of Energy's Office of Electricity and performed under the auspices of the U.S. Department of Energy by Lawrence Livermore National Laboratory under Contract DEAC52-07NA27344 with IM release number LLNL-JRNL-819834. The authors would like to thank Chloe Applegate, Emma Stewart, and Peter Barnes at Lawrence Livermore National Laboratory for providing technical support.

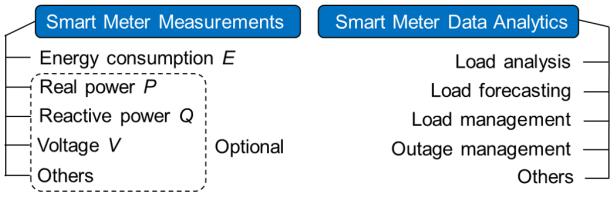

Fig. 1. Smart meter measurements and applications: A brief review.

categories to control categories, enabling smart meters' two-way communication feature being fully utilized.

Voltage monitoring and control is one of the most likely new applications. First, smart meters adopt voltage and currant transducers to measure energy consumption yielding an inherent voltage monitoring capacity. Second, smart meters allow two-way communication, enabling sending and receiving control commands in real-time or near real-time. Moreover, the voltage monitoring and control application can provide a new direction to address voltage stability issues. Traditionally, we maintain voltage stability through controlling the power system impedance at transmission sides [7]. While theoretically, we can also mitigate voltage instability at end-user sides if end-users could provide sufficient real and reactive power potentials with observability and controllability [8]. The latter is becoming promising as nowadays increasing amounts of distributed energy resources (DERs) and controllable loads are available at the power grid edge. For example, the California solar mandate, effective on January 1, 2020, requires new construction homes to have a solar photovoltaic (PV) system as an electricity source. Many DERs, such as PVs, can produce both real and reactive power through controlling 4-quadrant smart inverters [9]. Most controllable loads, such as heating, ventilation, and air conditioning (HVAC), can reduce their energy consumption adaptively according to demand response programs [10]. Therefore, integrating the voltage monitoring and control feature in smart meters will not only enhance the situational awareness at the grid edge, such as DERs and controllable loads, but also enable the voltage stability at the end-user side, i.e., the "last-mile" segment.

However, there are challenges ahead. First, smart meters, together with the communication network and meter data management system, constitute the advanced metering infrastructure (AMI). For the historically passive nature of power distribution systems, most utilities invested the AMI communication network with limited bandwidth, and chose to only record energy consumption in near real-time, such as in every 15/30/60 min [5]. There is few research specifying the impact of adding voltage measurements to smart meter datasets, especially in the communication perspective [1]–[5].

Second, even though several recent papers proposed voltage stability control solutions using smart meter measurements and DERs, their control objective focuses on the voltage magnitude only. For example, in the Volt/Var optimization (VVO), the control objective is to maintain the voltage magnitude within a standard range (e.g., 0.9-1.05 p.u. according to ANSI C84.1 standard) [11], [12]. In reality, the voltage magnitude is not a reliable indicator for voltage stability issues [13]. Excessive studies show that only controlling the voltage magnitude could lead to voltage collapse and even system-level faults [13]–[15]. For instance, Fig. 2 shows the PV curves at two locations in a feeder. The voltage magnitude threshold 0.9 p.u. cannot alert power system operators about the small stability margin appearing at location B. Without proper mitigation actions, potential voltage collapse could happen at location B.

Moreover, in the literature, most voltage stability control schemes via DERs are designed from the utility perspective, deploying utility-scale DERs for voltage regulation [16]. In practice, utility-scale DERs are only available at limited locations, and they are in need of considerable costs to enable the voltage regulation capability, such as the hardware and software investment [17]. To this end, several papers proposed the voltage control schemes using customer-owned DERs for their wider availability and lower cost [18]–[20]. Those schemes normally measure the voltage with DERs themselves and control the voltage in a distributed manner. Nowadays, there is no existing communication infrastructure between the customer-owned DERs and utility control center [21]. It is still a demanding task to investigate new efficient voltage control schemes by customer-owned DERs, but enabling utility's visibility and controllability at the grid edge.

To tackle the challenges above, this work investigates the new voltage monitoring and control feature for smart meters, and identifies the impact of this feature on both power distribution and communication systems. Specifically:

In terms of the voltage monitoring, the risk-benefit analysis for adding voltage measurements to smart meter outputs is presented, and the risk mitigation strategies along with the co-simulation validation using GridLAB-D and ns-3 are proposed. It is found that adding voltage measurements to smart meter readings has small impact on the AMI communication network, and the mitigation strategies can efficiently reduce timeout errors and packet drops for smart meter data.

In terms of the voltage control, a new voltage stability control scheme is developed, which applies the voltage stability margin as the control objective, instead of the traditional voltage magnitude. The proposed control scheme makes use of existing AMI and DERs, requiring small marginal costs. In particular, the proposed control scheme enables the voltage stability issues being solved at the grid edge, i.e. the "last-mile" segment, and also enhances the utility's observability and controllability at the grid edge.

Further, through integrating the voltage monitoring and control feature, the smart meter can provide additional values to utilities and customers. The co-simulation results imply that this new feature could support the coordination of the local and system-level voltage controls using both customer-owned and utility-scale DERs. This is the first work that considers voltage monitoring and control collectively for smart meter investment. The results can help the power engineering community supplement smart meter applications and shape the next-generation smart meters.

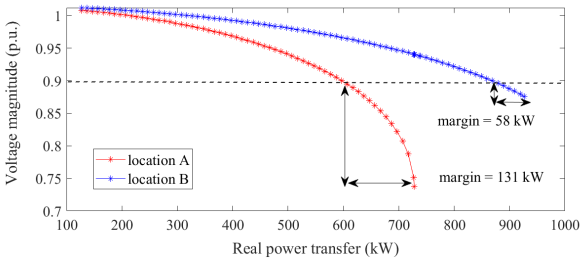

Fig. 2. Real power transfer margins at locations with different PV curves.

The remainder of this paper is organized as follows: Section II discusses the voltage monitoring issues and the corresponding mitigation strategies; Sections III describes the proposed voltage stability control schemes; and Sections IV and V validate the proposed solutions with the co-simulation platform and case studies. Finally, Section VI draws conclusions and discusses future work.

II. Voltage Monitoring

As aforementioned, smart meters have the inherent capacity for voltage monitoring. The voltage measurements can support various distribution-level applications, such as outage monitoring, voltage stability assessment, and VVO. Regardless, many utilities still choose to disable the voltage measurement channel in their smart meters. For example, according to the U.S. Department of Energy report, 32% of surveyed power utilities did not support voltage monitoring in their AMI [22].

A major reason is that adding new measurements to smart meter datasets will increase the payload size, which may lead to timeout errors and even package drops in terms of the limited bandwidth of AMI networks. This analysis is also true for low-rate wireless personal area networks (LR-WPANs), which are defined as AMI communication networks in IEEE 802.15.4 standard. Actually, many emerging technologies can reduce the risk caused by the increased payload size.

The risk can be mitigated through re-routing communication paths of smart meters. Since most AMI networks are configured as a meshed network, some meters may play a role as communication hubs to forward meter reading messages from downstream meters to the head end (i.e., cell relay). The increased packet size may prolong the processing time and cause the timeout error for other messages in the queue. Thus, re-planning the communication paths to avoid tremendous messages run into the same meter can improve the communication performance. Note that this method requires the AMI network with flexibility, which means that a meter should have multiple choices for selecting a parent/child node.

In addition, the risk can also be mitigated through re-configuring message sending patterns. Depending on the data usage, we can adjust the sending patterns or sending properties to reduce the network traffic. For example, enlarging the

sending time window and randomizing sending time for each node, increasing the sending time interval, decreasing the resolution of the data, etc.

This study assumes the data exchange between a smart meter and its local inverter is facilitated by a home area network (HAN). Although the inverters inherently measure their terminal voltage, it is still advantageous to employ smart meters to measure voltage. First, we can make use of the existing AMI system to enable the communications between the smart meter and the utility control center. Second, we can extend our approach from the inverter to other actuators (e.g., controllable loads) for voltage instability mitigation. Due to the limited space, the HAN is not thoroughly discussed in this study. It can be a follow-up research direction to this study.

III. Voltage Control

The voltage stability issue is one of the most fundamental problems in power engineering. It is traditionally formulated for bulk power systems, and its solutions have evolved from model-based control schemes to measurement-based control schemes [13]. In power distribution systems, the model-based control scheme is challenging since accurate and complete distribution models, especially end-user load composition models, are hard to obtain. Thus, this paper focuses on the measurement-based control scheme at the grid edge.

A. Control Objective

The traditional measurement-based control schemes are targeted at maintaining the voltage magnitude in a standard range. In contrast, the proposed control scheme is aimed at achieving the maximum voltage stability margin.

Originally, the voltage stability margin concept is proposed for the voltage stability in bulk power systems [23], [24]. It requires reactive power compensation equipment to be installed in bulk power systems with considerable cost and complexity [25]. Comparing to the voltage magnitude, the voltage stability margin presents to be a more reliable indicator for voltage stability. This is because the nature of voltage stability issues is the power flow solution reaching the nose point of PV curves, and the real power transfer margin, rather than the voltage magnitude, can better reflect the actual distance between the operation points of power flows and voltage collapses.

The proposed control scheme applies the voltage stability margin concept for voltage stability at the grid edge, making use of the existing real and reactive power resources at end-user sides, without installing new power equipment. The voltage stability margin can be estimated in the following way.

First, adopting Thevenin Equivalent (TE) theory to model electricity end-users as split-phase loads. In power distribution systems, each end-user is connected to a service transformer through a split-phase circuit. As shown in Fig. 3, a customer load is connected to a center tapped transformer, where $|V_1| = |V_2|$ and V_1 and V_2 have a phase difference of 180 degree.

Assuming smart meters support voltage monitoring, the split phase voltage measurements V_1, V_2 and current measurements I_{s1}, I_{s2}, I_{s12} can be obtained from smart meters. The load apparent power S_L can be calculated as

$$S_L = (V_1 - V_N)I_{s1}^* + (V_N - V_2)I_{s2}^* + (V_1 - V_2)I_{s12}^* \quad (1)$$

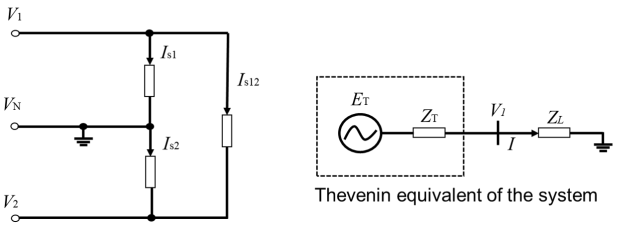

Fig. 3. Electricity end-user circuits: (a) Split-phase load circuits, (b) Thevenin equivalent circuits.

As $V_2 = -V_1$ and $V_N = 0$, we rewrite (1) as

$$S_L = V_1 I^* \quad (2)$$

$$I = I_{s1} + I_{s2} + 2I_{s12} \quad (3)$$

If following other standards rather than the split-phase standard in the U.S., the formulation of the apparent load can be slightly modified. For example, in the single-phase standard [26], (1)-(3) can be simplified to (2) with the line-to-neutral voltage and the current flowing through the hot wire.

Next, according to TE theory, a power system can be represented by Thevenin voltage and impedance as shown in Fig. 3. Technically, Thevenin voltage $E_T = E_{T,re} + jE_{T,im}$ and Thevenin impedance $Z_T = R_T + jX_T$ can be estimated through Kalman Filter (KF) using voltage measurements $V_1 = V_{1,re} + jV_{1,im}$, current measurements $I = I_{re} + jI_{im}$, and their measurement errors $\mathbf{e}$ in the following way.

$$\mathbf{z} = \mathbf{H}\mathbf{x} + \mathbf{e} \quad (4)$$

$$\mathbf{z} = \begin{bmatrix} V_{1,re} & V_{1,im} \end{bmatrix}^T \quad (5)$$

$$\mathbf{H} = \begin{bmatrix} 1 & 0 & -I_{re} & I_{im} \\ 0 & 1 & -I_{im} & -I_{re} \end{bmatrix} \quad (6)$$

$$\mathbf{x} = \begin{bmatrix} E_{T,re} & E_{T,im} & R_T & X_T \end{bmatrix}^T \quad (7)$$

The voltage and impedance in $\mathbf{x}$ can be estimated at each discrete time step t, which can be expressed as

$$\mathbf{P}_t = (\mathbf{I} - \mathbf{K}_t\mathbf{H}_t)\mathbf{P}_{t-1} \quad (8)$$

$$\mathbf{K}_t = \mathbf{P}_t\mathbf{H}_t^T\mathbf{R}_t^{-1} \quad (9)$$

$$\mathbf{x}_t = \mathbf{x}_{t-1} + \mathbf{K}_t(\mathbf{z}_t - \mathbf{H}_t\mathbf{x}_{t-1}) \quad (10)$$

where $\mathbf{R}$ is the covariance matrix of the measurement error.

Note that the KF algorithm above needs the voltage-phasor measurement. This can be implemented through integrating a phasor estimation algorithm in a smart meter [27]. For instance, a hardware implementation study is proposed in [28], which deploys a low-cost computation unit (average cost $13) in a smart meter to achieve the phasor estimation goal.

Theoretically, when Thevenin impedance Z_T equals to the load apparent impedance Z_L, we can achieve the maximum real power transfer from the service transformer to the household [29]. Therefore, the maximum real power transfer can be calculated as

$$P_{max} = \frac{|E_T|^2|Y_T|cos\phi}{2[1 + cos(\phi + \beta)]} \quad (11)$$

where ϕ is the load apparent power phase angle, $cos\phi$ is the load power factor, Y_T is the Thevenin admittance (i.e. $1/Z_T$), and β is the angle of Y_T.

As a result, the real power transfer margin can be determined by the maximum real power transfer P_{max} and the load real power P_L as

$$P_{margin} = P_{max} - P_L \tag{12}$$

Here, the real power transfer margin is selected as an indicator to execute voltage stability control schemes. It can indicate the maximum real power that can be transferred to an electricity end-user without causing voltage instability (i.e., voltage stability margin).

To further assess the voltage stability at the grid edge (e.g., the risk of end-users suffering voltage instability), an index is proposed as follows

$$\eta = \frac{1}{N_t} \sum_{t=0}^{N_t-1} \frac{P_{L,t}}{P_{max,t}} \tag{13}$$

The index η is represented by a ratio between the real power load and the maximum real power transfer limit from a service transformer to an end-user, in an assessment period comprising N_t meter readings. The index η smaller than "1" reflects a sufficient real power transfer margin. The smaller η refers to the larger voltage stability margin. In practice, the maximum real power transfer limit could fluctuate as it is estimated using measurement data. To this end, the average value over an assessment period is recommended.

B. Voltage Stability Control Scheme

Real power control and reactive power compensation are two common methods for voltage stability issues. This work focuses on the later since DERs and four-quadrant inverters are becoming increasingly available in distribution networks.

Here, a reactive power support approach is proposed for voltage stability control at the grid edge, when the stability index is estimated to be larger than an allowed threshold. With properly calculated reactive power support, the power flow solution at an end-user could be moved away from the voltage stability boundary [30]. The proposed approach is different from the other end-user level reactive power controls that aim at minimizing network loss and improving power quality [31], [32]. Instead of using local net reactive power and voltage deviation as control objectives, the proposed approach controls the real power transfer margin.

To achieve the maximum real power transfer, we need to work out the maximum real power margin and the corresponding reactive power support from end-users. This can be defined as an optimization problem that seeks the power factor of net load ϕ of an end-user that maximizes the objective P_{margin}. Here, ϕ is selected as the optimization variable because other variables in (11) are estimated from TE. Those variables depend on the system parameters external to the interested end-user. Thus, they can not be influenced by the end-user.

Typically, the maximum real power margin can be calculated using the partial derivative of P_{margin} with respect to the load apparent power phase angle ϕ

$$\frac{\partial P_{margin}}{\partial \phi} = \frac{|E_T|^2|Y_T|}{2} \frac{sin\beta - sin\phi}{[1 + cos(\phi + \beta)]^2} \tag{14}$$

Then the maximum P_{margin} can be achieved when $\partial P_{margin}/\partial\phi = 0$, in which $\phi = \beta$ is a solution.

With a rooftop PV installation, $P_L + jQ_L$ can be reinterpreted as the apparent netload of an end-user. The value of ϕ can be adjusted by leveraging the four-quadrant control mode of solar inverters. Within the inverter capacity S_{cap}, in order to achieve the maximum P_{margin}, the required reactive power support Q_{PV} can be calculated as

$$Q_{PV} = \begin{cases} Q_L - (P_L - P_{PV})tan\beta, & |P_{PV} + jQ_{PV}| \leq S_{cap} \\ (S_{cap}^2 - P_{PV}^2)^{1/2}, & \text{Otherwise} \end{cases} \tag{15}$$

Note that the inverter control logic is designed under the assumption that the end-user level solar inverters do not participate in the centralized VVO aiming at minimizing voltage violations in distribution systems. Hence, they do not receive commands from centralized controllers. Unlike VVO-based voltage regulation approaches [33] that only minimize voltage magnitude violation which could be deceptive regarding the distance from the actual stability boundary, the proposed approach controls the real power transfer margin. If not based on the stability boundary, voltage magnitude control could result in over-optimistic voltage stability assessment, which could potentially lead to voltage collapses. Due to the limited space, the interaction between the traditional VVO commands and the proposed controls will be studied in future work.

C. Voltage Stability Proactive Control Scheme

The real power transfer margin estimated in real time may not reflect the fast changing load condition of end-users. Similarly, the power factor control signal based on previous estimation may be outdated. In this case, forecast models would enable look-ahead stability margin estimation and proactive control on behind-the-meter DERs. An autoregressive integrated moving average (ARIMA) model is used in [34] to model the end-user electricity usage. The same forecast model structure can be applied to measurements $\{M_t : t \in T\}$, where T is the time index set. For this application, seven forecast models are fitted for $V_{1,re}$, $V_{1,im}$, $I_{s1,re} + I_{s12,re}$, $I_{s1,im} + I_{s12,im}$,$I_{s2,re} + I_{s12,re}$, $I_{s2,im} + I_{s12,im}$, P_{PV}. Those direct measurements are chosen is because they directly reflect the end-user behavior statistically. On the other hand, estimated quantities such as P_{margin} and β have a mixture of influences from the local end-user behavior, neighbouring end-user behavior, and Kalman filter, and thus are difficult to be fitted to low-order ARIMA models. Comparing with other complex surrogate models, ARIMA models have advantages on the low computation complexity and small size. These features very fit smart meter applications because of smart meters' constraints on limited computing power and memory space. The ARIMA model details can be found in Appendix.

IV. Co-simulation Development

To simulate the proposed voltage monitoring, control, and communication via smart meters in a scalable way, a co-simulation platform is developed. An illustrative diagram of the co-simulation platform is shown in Fig. 4.

The co-simulation platform couples the proposed models and algorithms implemented in Python with the triplex meter objects in GridLAB-D [35] and ns-3 [36]. The coupling mechanism is handled through the hierarchical engine for large-scale infrastructure co-simulation (HELICS) [37]. The voltage and current measurements are defined as publications subscribed by the real power transfer margin estimation algorithm. When the predictive estimation and control are enabled, solar inverter's real power output is published to the solar forecast algorithm. The inverter objects in GridLAB-D subscribe to power factor commands from the inverter control algorithm. The predictive module is implemented using Python package statsmodels [38]. All the software dependencies are managed using Spack [39], an open-source flexible package manager.

The co-simulation platform can simulate both the power distribution system (including the distribution substation, feeder, transformer, and house), the AMI communication network (involving the data center, cell relay, and smart meter), and their interactions. Here, IEEE 13-node feeder with 629 houses as shown in Fig. 5 is selected as the test system. The mapping of the nodes and houses and the mapping of the nodes, cell relays, and smart meters are summarized in TABLE I and TABLE II, respectively. In particular, each house is connected to a 4.16kV node through a 4.16kV/240V transformer and a triplex meter. Each customer load comprises cooling and heating, water heater, and ZIP loads (representing lighting).

TABLE I
Mapping of Nodes and Houses

Node	Phase-number of houses	Node	Phase-number of houses
632	A-2, B-6, C-10	652	A-41
671	A-62, B-59, C-71	634	A-1, B-4, C-5
675	A-73, B-112, C-70	692	A-52, B-10, C-5
645	B-21	646	B-18
611	C-7		

TABLE II
Mapping of Cell Relays, Smart Meters, and Distribution Nodes

Cell relay ID	Smart meter ID	Node
0	0 - 17	632
1	18 - 58	652
2	59 - 250	671
3	251 - 260	634
4	261 - 515	675
5	516 - 582	692
6	583 - 603	645
7	604 - 621	646
8	622 - 628	611

The schedule of cooling, heating, water tank, and lighting set points are randomized across all customers. The customer loads are modeled with the house object in GridLAB-D.

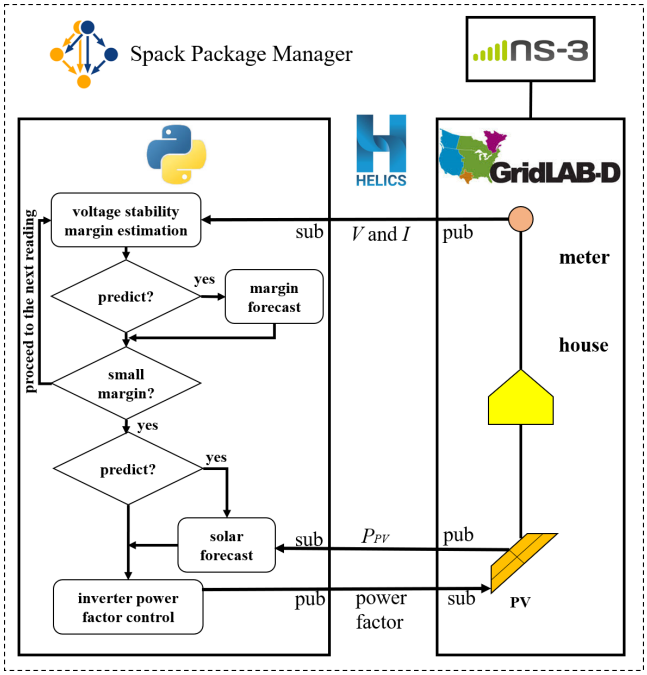

Fig. 4. Co-simulation platform for voltage monitoring, control, and communication via GridLAB-D, ns-3, and HELICS.

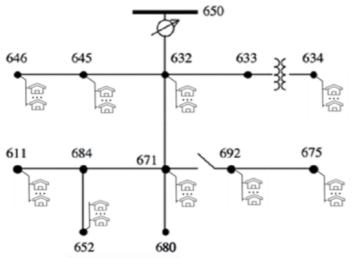

Fig. 5. Co-simulation test system: IEEE 13-node feeder with 629 houses.

V. Case Studies

In this section, a set of case studies is carried on the HELICS co-simulation platform and IEEE 13-node feeder test system to verify the performances of the proposed methods.

A. Voltage Monitoring Impact on AMI Network

To study the impact of adding voltage measurements to smart meter messages, a fictitious AMI communication network is simulated by ns-3 simulator.

TABLE III
Test Results of The Proposed Mitigation Strategies

Sending time window (sec)	Packet loss rate of full system (%)
10 (base case)	8.24
11	6.05
12	4.54
13	3.93
14	3.39
15	2.82
16	2.44
17	2.20

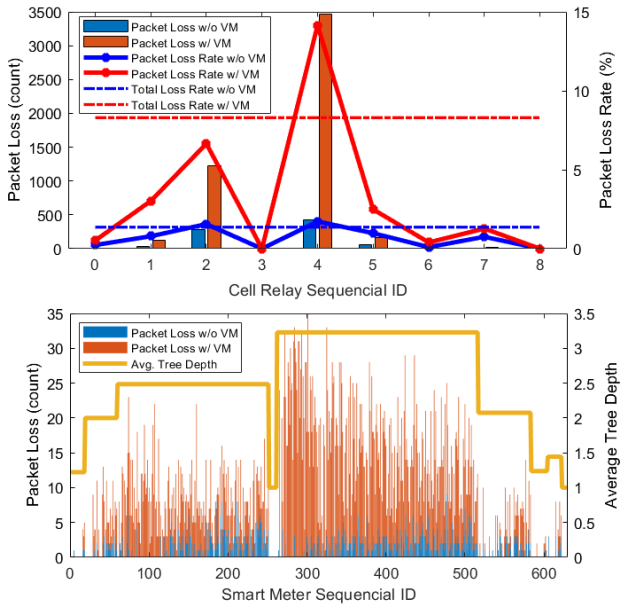

Fig. 6. AMI network performances w/ and w/o voltage readings.

In this fictitious network, following up TABLE II, 629 smart meters are connected to nine cell relays, and the nine cell relays are configured on nine responding distribution nodes, respectively. In the simulation, a 15-minute reading interval is selected for smart meter setting, since this time interval is increasingly deployed by utilities and the shorter time interval is favorable for advanced applications, such as demand response programs [22].

First, we test the AMI network performances without and with voltage measurements. The simulation results are shown in Fig. 6. It is observed that in most cell relays, the packet loss rates increase slightly after enabling the voltage monitoring feature. Cell relays 2 and 4 suffer greater impact due to their connecting with more smart meters with more complex connectivity. Note that the network complexity is measured by the average tree depth of a cell relay, which means the average message hops traveling from each meter to a cell relay.

As discussed in Section II, the impact can be mitigated through re-configuring message sending patterns. To this end, we test the AMI network performances under different message sending patterns. In the base case, all the smart meters are required to send the messages within 10 sec right after the scheduled data polling in every 15 minutes, and in the other cases, the smart meters are required with incremental sending time windows. The test results are shown in TABLE III. It is observed that when the sending time window increases slightly, the packet loss rate for the total nine cell relays is improved significantly. In particular, when the sending time window increases to 17 sec, the total package loss rate decreases to 2.2%, which is very close to the rate 2.0% (i.e. Total Loss Rate W/o VM in Fig. 6). Therefore, the test results suggest that adding voltage measurements to smart meter readings has small impact on the AMI network, and the emerging mitigation strategies can efficiently reduce timeout errors and packet drops for smart meter data.

B. Stability Margin Estimation

Next, we test the proposed stability margin estimation algorithm. Each house's real power transfer margin is estimated by the voltage and current measurements collected from the local triplex meter. Due to the limited space, the estimation results for a phase-A house at node 652, a phase-B house at node 645 and a phase-C house at node 671 are selected and shown in Fig. 7. It is observed that the margin between the maximum real power transfer and the actual real power consumed by the customers becomes very small multiple times a day. There are also several interesting findings as explained below.

Fig. 7(a) shows that the node-652 voltage decreases significantly below 115V around 4PM when most loads in the feeder reach their peaks. This is partially because node 652 is at the edge of the feeder (i.e. far away from the substation). Also, the current measurements in Fig. 7(a) suggest that the dominant load component for this household is cooling/heating which periodically activates to maintain the indoor temperature. The estimated real power transfer margin reflects this characteristic and fluctuates drastically through the day.

Fig. 7(b) describes a load profile with a different characteristic. From the current measurements, it can be observed that the ZIP load component (i.e. lighting) in this household takes a bigger percentage than the household in Fig. 7(a). Hence, the total load has a relatively large base value defined by the lighting load and fluctuations due to cooling/heating loads. Also, this household load is well maintained below the real power transfer limit except at 12PM, when the cooling/heating systems operate more frequently.

In addition, 7(c) also demonstrates a different load profile with a unique pattern. From the current measurements, multiple spikes can be found through the day. This household has a higher percentage of water heater load. The water heater operation will lead to temporary spikes in current measurements.

Those different load profiles contribute to the diversity of customer behaviors in a real power grid. For such diverse load profiles, aggregated real power transfer margin estimation is unable to capture all the granular indications of voltage instability. In this case, the proposed approach is helpful for filling this situational awareness gap.

C. Voltage Stability Control

With the actionable information provided by the stability margin estimation algorithm, the proposed pin-pointed inverter based voltage stability control scheme can be implemented. When the real power transfer margin is smaller than a predefined threshold, the proposed control scheme calculates the most effective Var support value to maximize the real power transfer limit. The Var support is then actuated though a power factor setpoint command sent to the inverter.

Fig. 8 shows the baseline voltage stability indices at 629 houses in different seasons. In spring and fall, the voltage stability indices at most houses are below 0.5, while in summer and winter, when the HVAC and water heaters are heavily used, the indices shift to large values. Note that the index is calculated with the TE algorithm and KF estimation,

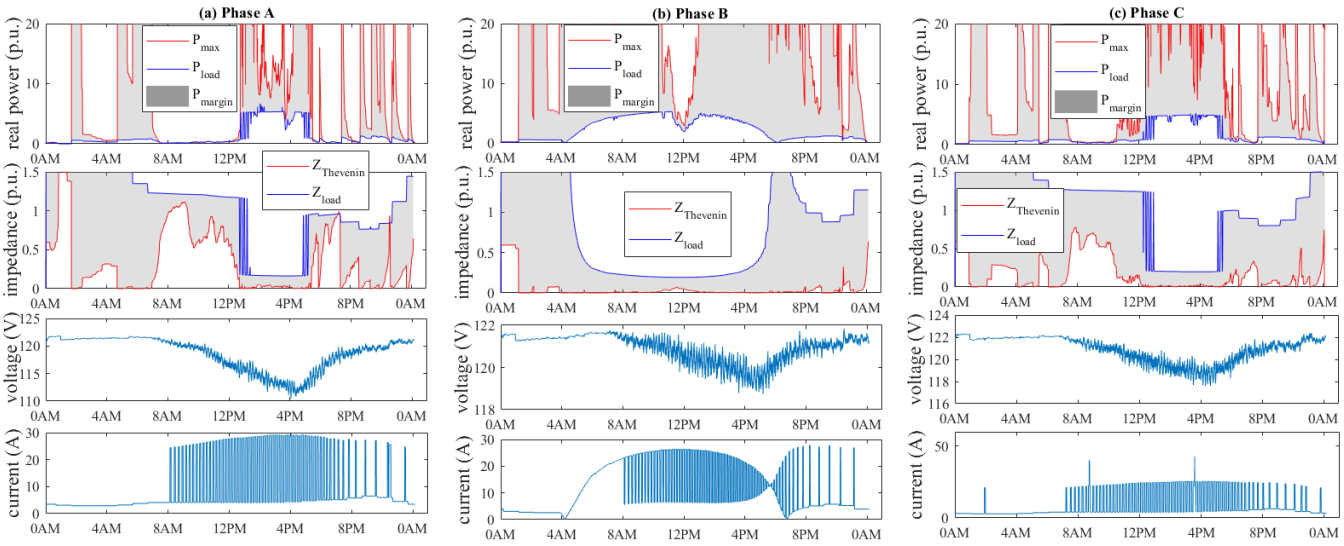

Fig. 7. Estimation results: (a) Phase A house at downstream of node 652 (b) Phase B house at downstream of node 645 (c) Phase C house at downstream of node 671. The four rows show the margin between the maximum real power transfer and the actual real power consumed by the customer, the margin between the estimated TE impedance and the load impedance, the voltage measurements, the current measurements, respectively.

which are subject to numerical limitations and estimation errors, respectively. Thus, the index larger than "1" does not necessarily imply instability, rather, it indicates the stability margin is smaller than the desired value and mitigation actions are required.

Fig. 9 shows the improved voltage stability index $\Delta\eta$ after applying the proposed voltage control scheme, as well as the numbers of the control signals sent from the meters to the inverters. It is observed that indices at most end-user sides are improved, where the maximum $\Delta\eta$ is 0.072 at meter 548 and the minimum $\Delta\eta$ is -0.05 at meter 368. After comparing the power factor control commands sent to meter 548 (most improved) and 368 (least improved) as shown in Fig. 10, we find an interesting result that although meter 368 sends much more control commands than meter 548, it is still unable to improve its voltage stability index. This phenomenon may implicate the limitation of local measurement-based voltage stability control. The coordination of local control and system-level control may achieve better results.

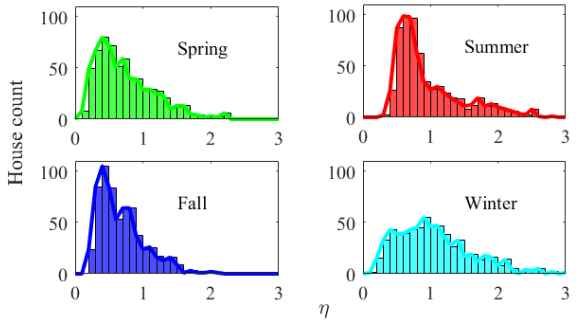

Fig. 8. Histogram of stability indices of 629 houses in different seasons.

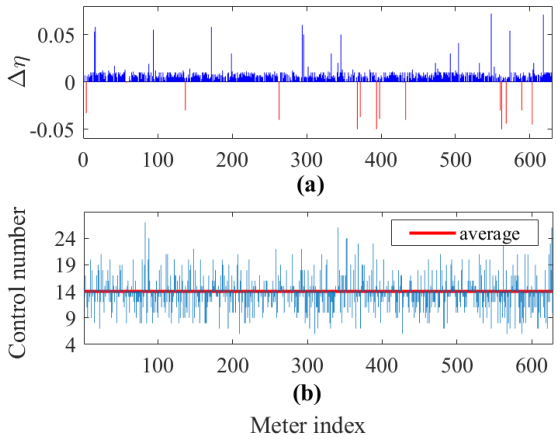

Fig. 9. Voltage stability control results: (a) Stability index improvement $\Delta\eta$ for all 629 houses; (b) Number of control signals sent to inverters.

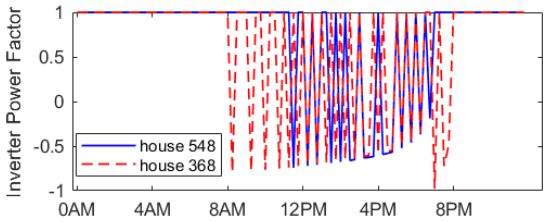

Fig. 10. Inverter power factor control signals for house 548 and 368.

D. Proactive Control

For the proposed proactive control, the prediction produced by the serialized ARIMA models are shown in Fig. 11. Here, the measurements from previous two days are used as the training data. A grid search approach is applied offline to identify the best-performance model orders. After the ARIMA models are trained, they are serialized with the Python Pickle

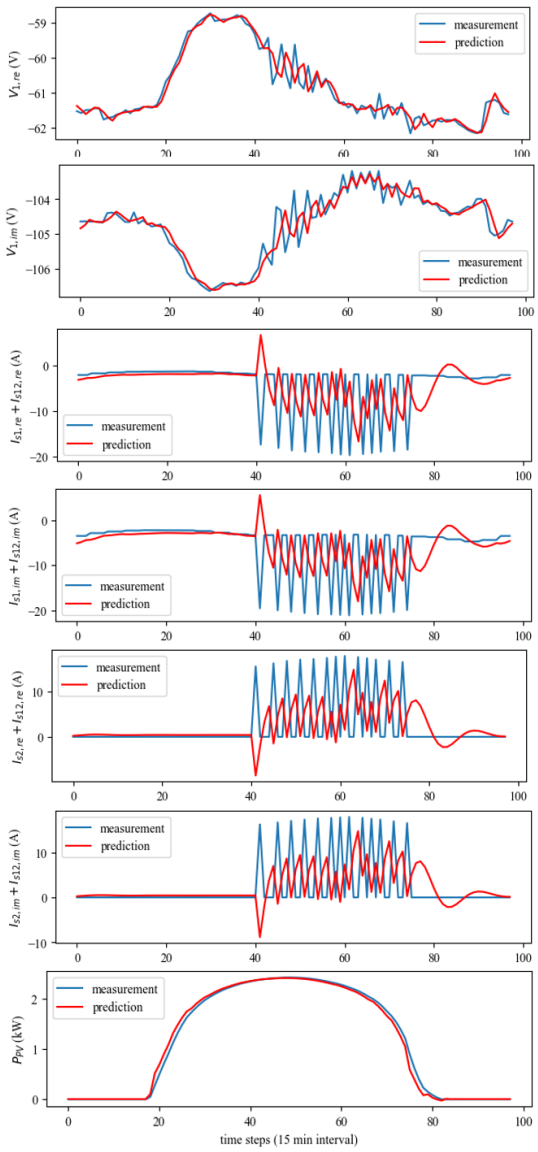

Fig. 11. Time series prediction using best-performance ARIMA models.

module. It is found that for measurements with a well-defined trend, such as voltage and inverter real power outputs, the ARIMA models produce better prediction comparing to the fast changing current measurements. Although the magnitudes of current measurement are not well captured, the models can still capture the cooling/heating systems' start/stop cadences throughout a 24-hour window. Without the predictive functionality, due to the outdated reactive power support commands, the average improvement of voltage stability index $\Delta\eta$ of all 629 houses is 0.0054. With the predictive functionality, it is improved to 0.0096. The advantage of the predictive approach can be better demonstrated if a FIDVR event is propagated from the bulk power grid, which requires co-simulation of both transmission and distribution systems [40].

E. Location Prioritization

In practice, transmitting voltage readings to the utility data center allows the utility to apply high-level control logic as an adjustment to local control logic. This is useful especially when there are high-level constraints that are challenging to be implemented locally.

For example, if the utility is constrained by user enrollment for reactive power support programs, it has to prioritize a certain number of locations for reactive power generation. In this case study, the centralized algorithm collects all voltage readings and ranks the calculated stability indices for all locations. If only a particular number of locations are allowed for reactive power generation, the utility selects the least stable locations to send control commands. The scenarios for prioritizing 100 and 200 locations are studied. The total reactive power generation at all nodes are shown in Fig. 12. It shows that as the number of prioritized locations increases, more reactive power is generated across all nodes.

The proposed approach also provides the flexibility to apply finer granularity changes at the end-user level. The different reactive power generation at houses downstream of node 675 phase B (the node and phase with the most customers) with different prioritization scenarios are shown in Fig. 13. It shows that when the number of locations allowed for reactive power generation changes, the contribution from each house also changes based on how unstable they are comparing to not only the houses under the same node but also those under other nodes in the network. This enables different levels of flexibility for reactive power support comparing to using a small number of utility-scale DERs.

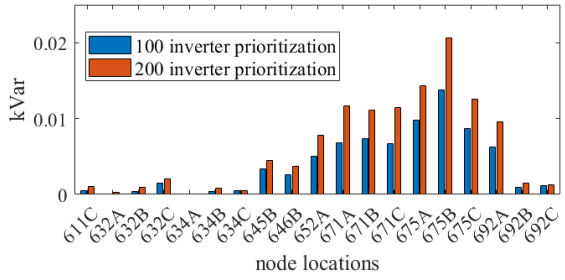

Fig. 12. Reactive power generation at the node level with different prioritization scenarios.

F. Computational Cost Analysis

The fast execution is critical for online applications. The execution time in TABLE IV suggests that both the real power transfer margin estimation and the reactive power support calculation can be completed within 1 ms. The ARIMA prediction takes relatively longer time but still around 79.9 ms. In this work, those algorithms are run on a laptop instead of a single-board computer. While considering those algorithms are only executed in a smart meter in every 15 minutes, the computational complexity should not be a limitation for their online applications.

VI. Conclusion

This work investigates the new voltage monitoring and control feature for smart meters, and identifies the impact of this feature on both power distribution and communication systems. Regarding the voltage monitoring, the risk-benefit

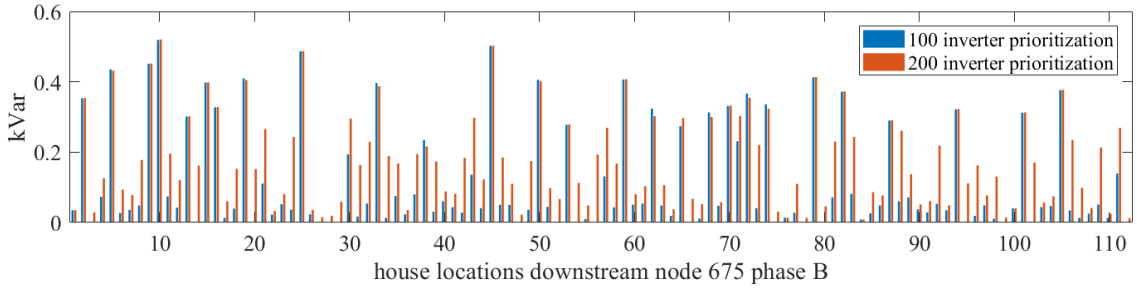

Fig. 13. Reactive power generation at the house level with different prioritization scenarios.

TABLE IV
AVERAGE TIME PERFORMANCE

Functionality	Average time (ms)
Voltage stability margin calculation	0.5
Var support calculation	0.2
ARIMA predition	79.9

analysis for adding voltage measurements to smart meter outputs is presented, and the risk mitigation strategies along with the co-simulation validation using GridLAB-D and ns-3 are proposed. It is found that adding voltage measurements to smart meter readings has small impact on the AMI communication network, and the mitigation strategies can efficiently reduce timeout errors and packet drops for smart meter data. Regarding the voltage control, a new voltage stability control scheme is developed, which applies the voltage stability margin as the control objective, instead of the traditional voltage magnitude. The proposed control scheme makes use of existing AMI and DERs, requiring small marginal costs.

Through integrating the voltage monitoring and control feature, smart meters can provide additional values to utilities and customers. To be specified, it is indicated that the feature could solve the voltage stability issues at end-user sides, i.e., the "last-mile" segment. It is also implied that the feature could support the coordination of the local and system-level voltage controls using both customer-owned and utility-scale DERS. This is the first work that considers voltage monitoring and control collectively for smart meters. The results can help the power engineering community supplement smart meter applications and shape the next-generation smart meters.

The future work could include investigating the interaction between residential-level margin-based reactive power support and utility-level VVO operations. Identifying the potential benefits of other optional smart meter measurements is also an interesting research topic.

APPENDIX
ARIMA MODEL

An ARIMA(p,d,q) model for $\{M_t : t \in T\}$ can be defined by three terms, including differentiation ∇^d, autoregression γ, and moving average θ [41]:

$$\gamma(B^p)\nabla^d M_t = \theta(B^q)Z_t \tag{16}$$

$$B^n M_t = M_{t-n} \tag{17}$$

$$\gamma(B^p) = 1 - \gamma_1 B - ... - \gamma_p B^p \tag{18}$$

$$\theta(B^q) = 1 + \theta_1 B + ... + \theta_q B^q \tag{19}$$

$$\nabla^d M_t = M_t - M_{t-d} \tag{20}$$

$$Z_t \sim N(0, \sigma_Z^2) \tag{21}$$

where p, d, q are the orders of auto-regression, differentiation and moving average terms respectively; B^n is the n-th order backshift operator; Z_t is white noise.

The offline training of an ARIMA model should be carried out periodically constrained by the memory of a smart meter. With locally stored historical data, the smart meter can update its ARIMA model before the historical data are removed for new recordings. Although smart meters have limited memory space (e.g., CENTRON meter has 256KB RAM and 512KB flash [42]), the implementation of the technology would potentially require connecting a single-board computer (e.g., BeagleBone Black with 512MB DDR3 RAM [43]) to the meter. The training task should be a local computing task with minimum communication traffic. The communication traffic this process could potentially generate is the command for resetting the training period, which will come from the utility.

REFERENCES

[1] D. Alahakoon and X. Yu, "Smart electricity meter data intelligence for future energy systems: A survey," *IEEE Trans. Industr. Inform.*, vol. 12, no. 1, pp. 425–436, 2016.
[2] Y. Wang, Q. Chen, T. Hong, and C. Kang, "Review of smart meter data analytics: Applications, methodologies, and challenges," *IEEE Trans. Smart Grid*, vol. 10, no. 3, pp. 3125–3148, 2019.
[3] N. Uribe-Pérez, L. Hernández, D. De la Vega, and I. Angulo, "State of the art and trends review of smart metering in electricity grid," *Appl. Sci.*, vol. 6, no. 68, pp. 1–24, 2016.
[4] A. Ghosal and M. Conti, "Key management systems for smart grid advanced metering infrastructure: A survey," *IEEE Commun. Surv.*, vol. 21, no. 3, pp. 2831–2848, 2019.
[5] S. Mihai *et al.*, "Next generation real-time smart meters for ICT based assessment of grid data inconsistencies," *Energies*, vol. 10, no. 7, p. 857–873, Jun 2017.
[6] J. Zhao, C. Huang, L. Mili, Y. Zhang, and L. Min, "Robust medium-voltage distribution system state estimation using multi-source data," in *2020 IEEE Power Energy Society Innovative Smart Grid Technologies Conference (ISGT)*, 2020, pp. 1–5.
[7] B. R. Williams, W. R. Schmus, and D. C. Dawson, "Transmission voltage recovery delayed by stalled air conditioner compressors," *IEEE Trans. Power Syst.*, vol. 7, no. 3, pp. 1173–1181, Aug 1992.
[8] J. A. Diaz de Leon and C. W. Taylor, "Understanding and solving short-term voltage stability problems," in *IEEE Power Engineering Society Summer Meeting,*, Chicago, IL, Jul 2002.

[9] W. Wang and F. de León, "Quantitative evaluation of DER smart inverters for the mitigation of fidvr in distribution systems," *IEEE Trans Power Del.*, vol. 35, no. 1, pp. 420–429, Feb 2020.

[10] F. A. Qayyum, M. Naeem, A. S. Khwaja, A. Anpalagan, L. Guan, and B. Venkatesh, "Appliance scheduling optimization in smart home networks," *IEEE Access*, vol. 3, pp. 2176 – 2190, Oct. 2015.

[11] H. Chen, W. Zhang, J. Lian, and A. J. Conejo, "Robust distributed volt/var control of distribution systems," in *2017 IEEE 56th Annual Conference on Decision and Control (CDC)*, Melbourne, Australia, Dec 2017, pp. 6321–6326.

[12] R. A. Jabr, "Robust volt/var control with photovoltaics," *IEEE Trans. Power Syst.*, vol. 34, no. 3, pp. 2401–2408, May 2019.

[13] F. Hu, K. Sun, A. D. Rosso, E. Farantatos, and N. B. Bhatt, "Measurement-based real-time voltage stability monitoring for load areas," *IEEE Trans. Power Syst.*, vol. 31, no. 4, pp. 2787–2798, Jul. 2016.

[14] K. Baker, A. Bernstein, E. Dall'Anese, and C. Zhao, "Network-cognizant voltage droop control for distribution grids," *IEEE Trans. Power Syst.*, vol. 33, no. 2, pp. 2098–2108, Aug 2018.

[15] D. Cao, W. Hu, J. Zhao, Q. Huang, Z. Chen, and F. Blaabjerg, "A multi-agent deep reinforcement learning based voltage regulation using coordinated pv inverters," *IEEE Trans. Power Syst.*, vol. 35, no. 5, pp. 4120–4123, Sep 2020.

[16] B. S. England and A. T. Alouani, "Real time voltage stability prediction of smart grid areas using smart meters data and improved thevenin estimates," *Int. J. of Elect. Power & Energy Syst.*, vol. 122, Nov 2020.

[17] K. A. Horowitz, Z. Peterson, M. H. Coddington, F. Ding, B. O. Sigrin, D. Saleem, S. E. Baldwin, B. Lydic, S. C. Stanfield, N. Enbar *et al.*, "An overview of distributed energy resource (DER) interconnection: Current practices and emerging solutions," National Renewable Energy Lab.(NREL), Golden, CO (United States), Tech. Rep., 2019.

[18] F. Ding, A. Pratt, T. Bialek, F. Bell, M. McCarty, K. Atef, A. Nagarajan, and P. Gotseff, "Voltage support study of smart PV inverters on a high-photovoltaic penetration utility distribution feeder," in *2016 IEEE 43rd Photovoltaic Specialists Conference (PVSC)*, 2016, pp. 1375–1380.

[19] L. Wang, R. Yan, and T. K. Saha, "Voltage regulation challenges with unbalanced PV integration in low voltage distribution systems and the corresponding solution," *Applied Energy*, vol. 256, p. 113927, 2019.

[20] P. Paudyal, F. Ding, S. Ghosh, M. Baggu, M. Symko-Davies, C. Bilby, and B. Hannegan, "The impact of behind-the-meter heterogeneous distributed energy resources on distribution grids," in *2020 47th IEEE Photovoltaic Specialists Conference (PVSC)*, 2020, pp. 0857–0862.

[21] O. R. Zinaman, T. Bowen, and A. Y. Aznar, "An overview of behind-the-meter solar-plus-storage regulatory design: Approaches and case studies to inform international applications," National Renewable Energy Lab.(NREL), Golden, CO (United States), Tech. Rep., 2020.

[22] The U.S. Department of Energy, *Advanced metering infrastructure and customer systems: results from the smart grid investment grant*, 2016.

[23] P. Zhang, L. Min, and N. Zhang, "Method for voltage instability load shedding using local measurements," U.S. Patent 11/539,758, Oct. 13, 2009.

[24] P. Zhang, L. Min, and J. Chen, "Measurement based voltage stability monitoring and control," U.S. Patent 12/131,997, Feb. 28, 2012.

[25] M. Nakmali, D. Osipov, and K. Sun, "A new hybrid approach to Thevenin equivalent estimation for voltage stability monitoring," in *IEEE Power & Energy Society General Meeting*, Denver, CO, Jul. 2015.

[26] IEEE, "IEEE standard for pad-mounted-type, self-cooled, single-phase distribution transformers 250 kVA and smaller: High voltage, 34 500 GrdY/19 920 V and below; low voltage, 480/240 V and below," *IEEE Std C57.12.38-2014 (Revision of IEEE Std C57.12.38-2009)*, pp. 1–36, 2014.

[27] K. R. Krishnanand, B. Prasad, Hoang Duc Chinh, A. K. Rathore, and S. K. Panda, "Smart-metering for monitoring building power distribution network using instantaneous phasor computations of electrical signals," in *IECON 2013 - 39th Annual Conference of the IEEE Industrial Electronics Society*, 2013, pp. 2180–2184.

[28] M. C. Garcia, D. Dotta, L. Pereira, M. C. d. Almeida, O. L. D. Santos, and L. C. P. da Silva, "Design and development of D-PMU module for smart meters," in *2020 IEEE Power Energy Society General Meeting (PESGM)*, 2020, pp. 1–5.

[29] K. Vu, M. M. Begovic, D. Novosel, and M. M. Saha, "Use of local measurements to estimate voltage-stability margin," *IEEE Trans. Power Syst.*, vol. 14, no. 3, pp. 1029–1035, Aug. 1999.

[30] F. Hu, L. Yang, J. Wang, Y. Ma, K. Sun, L. M. Tolbert, and F. Wang, "Measurement-based voltage stability assessment and control on curent hardware test bed system," in *IEEE Power and Energy Society General Meeting*, Boston, MA, Jul 2016.

[31] K. Turitsyn, P. Sulc, S. Backhaus, and M. Chertkov, "Local control of reactive power by distributed photovoltaic generators," in *2010 First IEEE International Conference on Smart Grid Communications*, 2010, pp. 79–84.

[32] ——, "Options for control of reactive power by distributed photovoltaic generators," *Proceedings of the IEEE*, vol. 99, no. 6, pp. 1063–1073, 2011.

[33] F. Bell, A. Nguyen, M. McCarty, K. Atef, and T. Bialek, "Secondary voltage and reactive power support via smart inverters on a high-penetration distributed photovoltaic circuit," in *IEEE Power & Energy Society Innovative Smart Grid Technologies Conference (ISGT)*, Minneapolis, MN, Sep. 2016.

[34] N. Duan, J. Cadena, P. Sotorrio, and J. Joo, "Collaborative inference of missing smart electric meter data for a building," in *IEEE 29th International Workshop on Machine Learning for Signal Processing (MLSP)*, Pittsburgh, PA, Oct 2019.

[35] D. P. Chassin, K. Schneider, and C. Gerkensmeyer, "GridLab-D: an open-source power systems modeling and simulation environment," in *IEEE Power & Energy Society T & D Conf. Expo.*, Chicago, IL, Apr. 2008.

[36] The ns-3 network simulator. [Online]. Available: http://www.nsnam.org/

[37] HELICS: Hierarchical engine for large-scale infrastructure co-simulation. [Online]. Available: https://www.helics.org/

[38] S. Seabold and J. Perktold, "Statsmodels: Econometric and statistical modeling with python," in *9th Python in Science Conference*, 2010.

[39] T. Gamblin, M. P. LeGendre, M. R. Collette, G. L. Lee, A. Moody, B. R. de Supinski, and W. S. Futral, "The Spack package manager: Bringing order to HPC software chaos." in *Supercomputing 2015 (SC'15)*, Austin, Texas, Nov 2015.

[40] N. Duan, C. Sun, R. Mast, P. Sotorrio, V. Donde, W. Ren, and I. Alvarez-Fernandez, "Parallel transmission distribution co-simulation leveraging a commercial distribution simulator," in *IEEE Power & Energy Society ISGT-Europe*, Delft, The Netherlands, Oct. 2020.

[41] D. Peter and S. Pastoreková, "ARIMA vs. ARIMAX–which approach is better to analyze and forecast macroeconomic time series," in *Proc. 30th International Conference Mathematical Methods in Economics*, Karviná, Czech Republic, Sep. 2012, pp. 136–140.

[42] "CENTRON GPRS SmartMeter data sheet," Itron, Liberty Lake, Washington.

[43] "BeagleBone Black open-source Linux computer unleashes innovation," White Paper, Texas Instruments, Aug. 2018.

Nan Duan (S'14–M'18–SM'20) received his B.S. in automation from Beijing University of Technology, Beijing, China, M.Eng. in control engineering from Beihang University, Beijing, China and Ph.D. in electrical engineering from the University of Tennessee, Knoxville, TN, USA, in 2010, 2013 and 2018, respectively. He is currently a power systems engineer with Lawrence Livermore National Laboratory, CA, USA. His research interests include power system modeling, high-performance computing, machine learning, and synchrophasor applications.

Can Huang (S'13–M'16–SM'18) received the B.S.E.E degree from Hohai University, Nanjing, China, in 2008, the M.S.E.E. degree from Southeast University, Nanjing, China, in 2011, and the Ph.D. degree in electrical engineering from the University of Tennessee, Knoxville, TN, USA, in 2016. Now he is a research staff with Lawrence Livermore National Laboratory, Livermore, CA, USA. His current research interests include smart sensors, data analytics, and machine learning for energy and power systems, cyber-physical systems, and Internet of Things.

Chih-Che Sun (S'15-M'20) received the Ph.D. degree in electrical engineering from the Washington State University, Pullman, WA, USA, in 2019. He is currently a postdoctoral research staff with Lawrence Livermore National Laboratory, Livermore, CA, USA. His current research interests include cyber-physical systems (CPS) security, and their modeling and simulation.

Liang Min (S'05–M'07–SM'12) received the B.S. and M.S. degrees from Tianjin University, Tianjin, China, in 2001 and 2004, respectively, and the Ph.D. degree from Texas A&M University, College Station, TX, USA, in 2007, all in electrical engineering. He is currently the managing director with the Bits & Watts initiative at Stanford University, CA, USA. His current research interests include the simulation and analysis of national critical infrastructure with a particular focus on energy infrastructure.